HAND (2010) 5:77–81
DOI 10.1007/s11552-009-9220-9

ORIGINAL ARTICLE

Morphological Analysis of the Carpal Tunnel

Corey A. Pacek · Jie Tang · Robert J. Goitz · Robert A. Kaufmann · Zong-Ming Li

Received: 22 April 2009 / Accepted: 12 August 2009 / Published online: 4 September 2009

Abstract Although carpal tunnel release is one of the most commonly performed procedures in the USA, the morphology of the carpal tunnel as determined previously in the literature has been questioned. Previous methodology has been questioned for accuracy by recent studies. The purpose of this study was to perform a morphological analysis of the carpal tunnel and correlate carpal tunnel and hand dimensions. The carpal tunnels of ten cadaveric specimens were emptied of their contents and a silicone cast of the carpal tunnel was then created. This cast was then digitized, and the dimensions of the carpal tunnel were calculated. These dimensions were compared with the measured hand dimensions of the specimens. The width, depth, tilt angle, length, cross-sectional area, and volume of the carpal tunnel were 19.2 ± 1.7 mm, 8.3 ± 0.9 mm, 14.8 ± 7.8°, 12.7 ± 2.5 mm, 134.9 ± 23.6 mm^2, and 1,737 ± 542 mm^3, respectively. Width, depth, and cross-sectional area did not change significantly along the length of the carpal tunnel, but tilt angle did. The width of the palm strongly correlates with the width of the carpal tunnel. Other dimensional correlations did not reach statistical significance. The carpal tunnel is of uniform dimension along its length. The long axis of the carpal tunnel in cross-section rotates volarly from the radial side of the hand increasingly with distal progression along the carpal tunnel. Based on our analysis of ten cadaveric specimens, the width of the carpal tunnel may be estimated by the width of the palm using the equation: $\text{Width}_{CT} = 1.285 + 0.236 \times \text{Width}_{palm}$.

Keywords Carpal tunnel · Carpal tunnel syndrome · Anatomy · Morphology

Introduction

Carpal tunnel syndrome (CTS) is one of the most common compression neuropathies in the USA today, with an incidence of approximately 3.7% [11]. Subsequently, carpal tunnel release is one of the most commonly performed surgical procedures, occurring between 400,000 and 500,000 times per year in the USA with an estimated direct cost of $2 billion [10]. CTS results from compression of the median nerve within the boundaries of the carpal tunnel through an uncertain etiology/mechanism.

The inner boundaries of the carpal tunnel are made up of soft tissues, either on the surface of the carpal bones at the radial, ulnar, and dorsal margins or the transverse carpal ligament (TCL) at the volar margin. These soft tissues can be imaged using magnetic resonance imaging (MRI), which has been the imaging modality of choice for study of carpal tunnel morphology [1, 7–9, 12–14].

Richman et al. [12] employed MRI as a means to measure carpal tunnel volume. They defined the proximal and distal edges of the carpal tunnel by the proximal and distal edges of the TCL. They compared MRI volumes with volumes determined by silicone casting of the carpal tunnel

Ethical Statement As this was a cadaveric study, all experimentations were performed following the approval by the University of Pittsburgh Committee for Oversight of Research Involving the Dead (CORID).

C. A. Pacek · J. Tang · R. J. Goitz · R. A. Kaufmann · Z.-M. Li
Hand Research Laboratory, Department of Orthopaedic Surgery, University of Pittsburgh,
Pittsburgh, PA 15213, USA

Z.-M. Li (✉)
210 Lothrop Street, BST E1641, Pittsburgh, PA 15213, USA
e-mail: zmli@pitt.edu

based on the known density of the cured silicone. The volumes between the two methods were found to be non-significantly different when a correction factor of 0.8161 was multiplied by the MRI volume. Cobb et al. [3] verified the work of Richman et al. using the same correction factor.

Skie et al. [13] measured average cross-sectional areas of the carpal tunnel at the level of the hook of hamate and found a mean of 152 mm^2. Allman et al. [1] found similar numbers in their MRI study, with mean cross-sectional areas of 152 mm^2 again at the level of the hamate and 178 mm^2 at the level of the pisiform. Cobb et al. [4] also found the carpal tunnel to be most narrow at the level of the hook of the hamate. In both of these papers, no correction factor was used with the MRI measurements. Other papers have also found the hamate to be the most narrow point of the carpal tunnel [7, 9, 14], but more recent literature has reported the opposite and found that the carpal tunnel had the greatest cross-sectional area at the level of the hamate [2].

Correction factor utilization for measuring carpal tunnel dimensions calls into question this method's accuracy. Two problems exist when using MRI images for acquiring measurements. The first problem is that defining the extent of the carpal tunnel by MRI relies on observer interpretation of these boundaries, which are typically not distinct, making the user-defined delineation difficult and inaccurate. The second problem is parallax error. A cross-sectional area measurement that is not perpendicular to the axis of a cylinder will be greater than the true cross-sectional area. Since the axis of the carpal tunnel cannot accurately be defined using external anatomical features of the hand or carpus, it is impossible to reliably align the axis of the carpal tunnel with the MRI coil. Mogk and Keir showed that external wrist position could not reliably be used for axis determination of the carpal tunnel and that off-axis cross-sectional area determinations did give false values [8]. Thus, the gold standard for measured volume for both Richman et al. and Cobb et al. studies was a poured cast of the carpal tunnel [3, 12]. At that time, however, dimensional analysis was limited using that method.

The purpose of this study was to perform a morphological analysis of the carpal tunnel using an advanced silicone casting and digitization method and correlate these data with external hand dimensions.

Materials and Methods

Ten cadaveric fresh-frozen hand specimens were used in this study. The experiment was performed in conjunction with our previously published study [15]. Briefly, dissection was carried out volarly to expose the flexor retinaculum (FR). The carpal tunnel was evacuated by removing the median nerve and flexor tendons. The carpal tunnel was created with a silicone molding technique. A local coordinate system was established by an aluminum plate, which was firmly molded with the silicone (Fig. 1). While the silicone was inside the carpal tunnel, bony landmarks and control points on the plate were digitized using a three-dimensional digitizer (Microscribe GX2, Immersion Corp., San Jose, CA, USA).

The carpal tunnel cast was then removed and the proximal excess sharply excised. The cast was then reattached to the apparatus using the boom (Fig. 2). The local coordinate system of the aluminum plate was again digitized, followed by the entire surface of the carpal tunnel cast.

Custom software (MATLAB, The MathWorks, Natick, MA, USA) was then used to reconstruct a surface based on the digitized data. The central axis of the carpal tunnel was then mathematically determined by creating a line through the centroid of multiple slices taken through the carpal tunnel. This central axis was then defined as the *y*-axis. The *x*-axis was determined by the projection of the line passing through the ridge of the trapezium and the hook of the hamate on the transverse plane perpendicular to the *y*-axis. The *z*-axis was finally defined as orthogonal to the *x*- and *y*-axis. The three-dimensional coordinates of the digitized data were then converted to this local coordinate system. The carpal tunnel was defined by the most distal point of

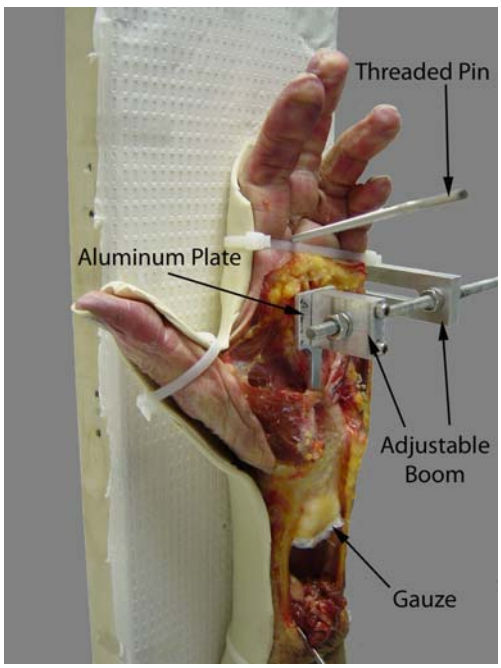

Figure 1 The specimen is dissected and attached to the apparatus ready for pouring of the cast of the carpal tunnel. The aluminum plate is positioned within the carpal tunnel without touching the sides and is firmly and stably attached to the boom.

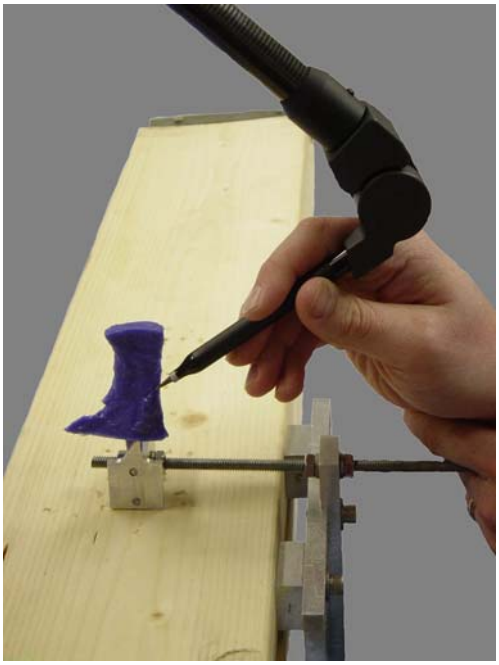

Figure 2 Reattachment of the cast of the carpal tunnel to the apparatus for digitization of its surface.

the proximal edge of the transverse carpal ligament to the most proximal point of the distal edge of the transverse carpal ligament. Eleven cross-sectional slices were made perpendicular to the axis of the carpal tunnel (*y*-axis) from 0% to 100% of the longitudinal direction of the carpal tunnel, with 0% representing the proximal extent. Within each slice, the surface points were interpolated and smoothed based on the digitized data to construct a maximum envelope. The long and short axes of this envelope were determined by principal component analyses. The definitions of the slice dimensions are illustrated in Fig. 3. The tilt angle of the slice was defined as the angle between the long axis of this ellipsoid slice and the *x*-axis. The width and depth of the slice were defined as the lengths of the two principal axes. The cross-sectional area of carpal tunnel was defined as the area of the maximum envelope.

Dimensions were then calculated for each cross-sectional slice of the carpal tunnel and include width, depth, tilt angle, and cross-sectional area. The length along the *y*-axis and volume of the carpal tunnel were calculated as well. Differences in measured hand dimensions and calculated carpal tunnel dimensions were evaluated with one-way repeated measures ANOVA using statistical software (SPSS Inc., Chicago, IL, USA). Correlation analysis was performed between hand and carpal tunnel dimensions. Once the correlation analysis was complete, a stepwise linear regression analysis was then performed using the carpal tunnel dimensions as the dependent variables and the hand dimensions as the independent variables to derive a linear regression equation.

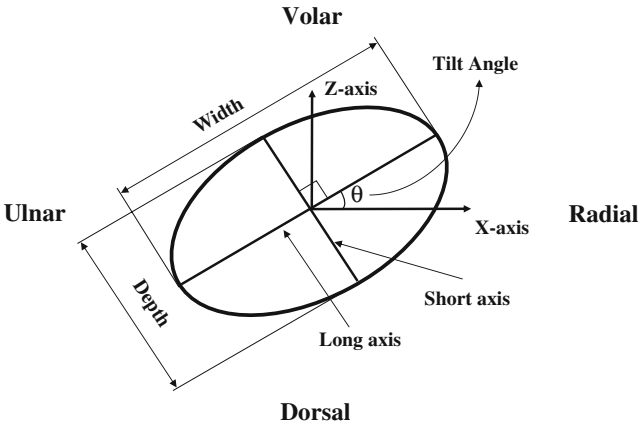

Figure 3 The carpal tunnel is approximated as an ellipse in this figure to illustrate the definitions of width, depth, and tilt angle of each carpal tunnel slice. Width was defined as the long axis of the ellipse, depth as the short axis, and tilt angle as the angle between the long axis of the ellipse and the *x*-axis. (Please refer to the text for definition of the *x*-axis.)

Results

An example of the reconstructed, digitized carpal tunnel silicone cast is shown in Fig. 4. The central axis was identified and found to be a straight line (*R*-square values). The width, depth, and cross-sectional area did not change significantly along the central (*y*) axis of the carpal tunnel (p=0.09, 0.836, and 0.475, respectively; Fig. 5). Hence, the mean values of the 11 slices were obtained for each specimen. The width and depth of the carpal tunnel were 19.2±1.7 and 8.3±0.9 mm, respectively, and the width to depth ratio was 2.3±0.2. The tilt angle was 14.8±7.8°. The tilt angle did change significantly along the length of the carpal tunnel, rotating away from the radial aspect of the hand distally (mean range 8.2–16.2°, $p<0.001$). The length of the carpal tunnel (defined by the TCL edges) was 12.7±2.5 mm. The cross-sectional area was 134.9±23.6 mm^2. The volume of the defined carpal tunnel was 1,737±542 mm^3.

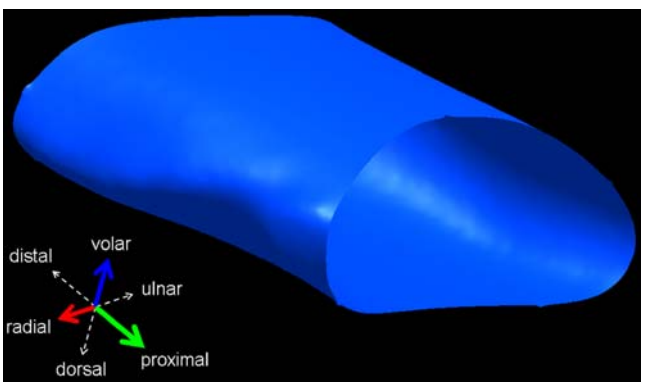

Figure 4 Three-dimensional reconstruction of the carpal tunnel of a left hand.

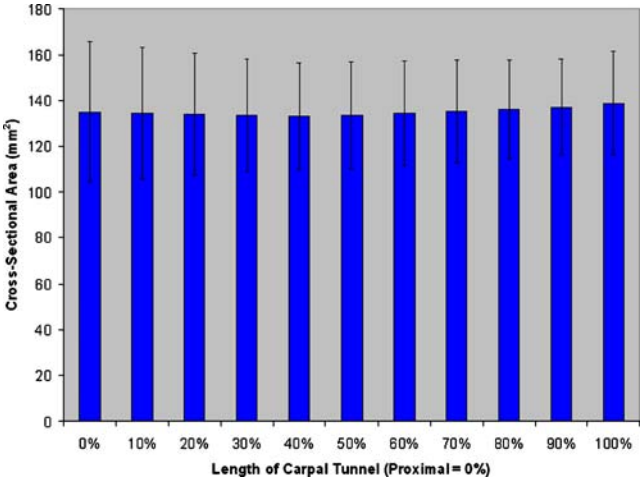

Figure 5 The cross-sectional areas of slices at 10% intervals along the carpal tunnel. The cross-sectional area does not significantly change along the length of the carpal tunnel.

Carpal tunnel width was found to positively correlate with wrist width ($p<0.05$, $r=0.632–0.749$), depth ($p<0.041$, $R=0.653–0.710$), and circumference ($p<0.049$, $r=0.635–0.703$) and palm width ($p<0.025$, $r=0.691–0.882$) and circumference ($p<0.047$, $r=0.638–0.736$). Following stepwise regression analysis, the resulting model ($\text{Width}_{CT} = 1.285 + 0.236 \times \text{Width}_{palm}$; $p<0.01$, $r=0.829$, $r^2=0.687$) included only palm width, as once the variance accounted for by this variable was removed, the remaining variance attributed to the other variables (wrist width, depth, circumference, and palm circumference) became non-significant. This was the only statistically significant linear regression equation that could be derived based on our data set. Carpal tunnel depth did not correlate with the measured hand dimensions (all $p>0.1$).

The male specimen hand dimensions were significantly larger than the female specimens with regards to wrist width ($p<0.001$), depth ($p<0.05$), and circumference ($p<0.001$), palm width ($p<0.01$), depth ($p<0.05$) and circumference ($p<0.01$), and hand volume ($p<0.05$). There was no significant difference between hand length of male and female specimens ($p=0.098$). Male specimens were found to have significantly larger carpal tunnel width and cross-sectional area ($p<0.0001$), and female specimens were found to have larger mean tilt angles ($p<0.0001$), but no significant differences were found with respect to depth and volume ($p=0.428$ and 0.120, respectively).

Discussion

The narrowest point of the carpal tunnel has previously been identified by MRI to be at the level of the hook of the hamate [3, 5, 7, 9, 14], but this has been questioned through more recent MRI studies [2]. We find that neither the width, nor depth, nor cross-sectional area changes significantly along the length of the carpal tunnel.

Cobb et al. [4] reported widths from radiographs of the carpal tunnel after injection with radio-opaque material as 24.7±1.2 mm proximally, 19.8±1.2 mm at the hook of the hamate, and 25.2±1.5 mm distally. They concluded that the narrowest point of the carpal tunnel was thus at the hook of the hamate, but did not report other widths within the carpal tunnel. Again, our data show no significant change in width along the length of the carpal tunnel. The distal measurement in their paper was actually measured at the edge of the distal aponeurotic portion of the FR, as opposed to the edge of the TCL as in this study. The proximal measurement was set at the proximal edge of the TCL. Although not specifically stated, if the most proximal portion of the proximal edge was chosen, part of the width would represent the area covered by the antebrachial fascia instead of the TCL and thus may not represent the true width of the carpal tunnel.

Our determination of length, 12.7±2.5 mm, is smaller than those determined by Cobb et al. of 21.7±6.05 mm [4]. This is, in part, secondary to our definition of the proximal and distal extents of the carpal tunnel. In our study, we used the most distal extent of the proximal border of the TCL and the most proximal extent of the distal border of the TCL, whereas Cobb et al. used the opposite and included the distal aponeurotic portion of the flexor retinaculum in the calculation as well. Calculation of the length of the carpal tunnel is thus dependent upon one's definition of the proximal and distal extents.

Cross-sectional areas between 150 and 350 mm^2 have also been reported[2]. One possible reason for this discrepancy is that the soft tissue borders of the carpal tunnel are difficult to distinguish on MRI. Since the bones are more easily visualized on MRI, the common error has been to define a region closer to the bone edges, leading to the measurement of a larger cross-sectional area. Larger cross-sectional areas would likewise be reported secondary to potential parallax error. These MRI inaccuracies may be causative for our average cross-sectional area of 135 mm^2 being smaller than what has previously been reported.

Likewise, our determined volume of the carpal tunnel, 1,737±542 mm^3, was also smaller than that determined by others of 3,000–4,000 mm^3 [12]. Since our defined length of the carpal tunnel was smaller, one would expect the resultant volume to be smaller as well. Thus the determination of volume is arbitrary based on the definition of the carpal tunnel. This makes comparison of our currently calculated values with those previously reported in the literature difficult.

The tilt angle of the carpal tunnel is a new concept. While our actual number is dependent on the defined coordinate system and is, in fact, arbitrary, the change in the

value is significant. Our data suggest that as one progresses distally in the carpal tunnel, the long axis of the cross-sectional slices of the carpal tunnel rotates away from the radial side of the hand. The carpal tunnel is essentially elliptical on cross-section, and when extruded longitudinally, the resultant cylinder is then rotated around the central axis in space. While this change in tilt angle is significant, its clinical relevance is yet to be determined. This rotation may lead to constraint of the tendons and nerves within the carpal tunnel during wrist motion. Further research is needed to identify whether or not individuals with higher or lower tilt angle are predisposed to the development of CTS.

The only significant correlation of hand and carpal tunnel dimensions was that between palm width and carpal tunnel width. Using regression analysis, we have developed a mathematical model ($\text{Width}_{CT} = 1.285 + 0.236 \times \text{Width}_{palm}$) that estimates carpal tunnel width using the width of the palm measured at the level of the metacarpal heads.

The etiology of CTS has yet to be identified, but smaller carpal tunnel size has been postulated as a possible contributing factor [1]. Using this formula, the size of the carpal tunnel can be estimated in the office in a quick and inexpensive manner. With further research into differences between carpal tunnel morphology, specifically that of tilt angle, of normal individuals and patients with CTS, this model may have utility in the evaluation and diagnosis of CTS.

This study has shown that females have carpal tunnels that are more narrow and with smaller cross-sectional areas when compared to males. In addition, female cadavers were found to have a greater tilt angle than male cadavers. A higher disposition towards CTS in females [6] may be related to these morphologic differences. Although females have been shown to have smaller carpal tunnels than men, the carpal tunnel contents have also been shown to be proportionally smaller in women [2]. Further research into the morphological differences between men and women with respect to both the carpal tunnel and its contents, as well as further research into the differences between patients with and without CTS, is necessary to further characterize the relationship of carpal tunnel morphology to carpal tunnel syndrome.

Acknowledgments The authors thank several people for their assistance: Matthew Chakan for the performance of experiments, Luke Xie for the three-dimensional figures, and Jay Irrgang, PhD, for the statistical analysis. The authors acknowledge the support from the National Institutes Health (NIH R03AR054510).

References

1. Allmann KH, Horch R, Uhl M, et al. MR imaging of the carpal tunnel. Eur J Radiol. 1997;25(2):141–5.
2. Bower JA, Stanisz GJ, Keir PJ. An MRI evaluation of carpal tunnel dimensions in healthy wrists: implications for carpal tunnel syndrome. Clin Biomech (Bristol, Avon). 2006;21(8):816–25.
3. Cobb TK, Dalley BK, Posteraro RH, et al. Establishment of carpal contents/canal ratio by means of magnetic resonance imaging. J Hand Surg [Am]. 1992;17(5):843–9.
4. Cobb TK, Dalley BK, Posteraro RH, et al. Anatomy of the flexor retinaculum. J Hand Surg [Am]. 1993;18(1):91–9.
5. Cobb TK, Bond JR, Cooney WP, et al. Assessment of the ratio of carpal contents to carpal tunnel volume in patients with carpal tunnel syndrome: a preliminary report. J Hand Surg [Am]. 1997;22(4):635–9.
6. Geoghegan JM, Clark DI, Bainbridge LC, et al. Risk factors in carpal tunnel syndrome. J Hand Surg [Br]. 2004;29:315–20.
7. Horch RE, Allmann KH, Laubenberger J, et al. Median nerve compression can be detected by magnetic resonance imaging of the carpal tunnel. Neurosurgery. 1997;41(1):76–82. discussion 82-73.
8. Mogk JP, Keir PJ. Evaluation of the carpal tunnel based on 3-D reconstruction from MRI. J Biomech. 2007;40:2222–9.
9. Monagle K, Dai G, Chu A, et al. Quantitative MR imaging of carpal tunnel syndrome. AJR Am J Roentgenol. 1999;172 (6):1581–6.
10. Palmer DH, Hanrahan LP. Social and economic costs of carpal tunnel surgery. Instr Course Lect. 1995;44:167–72.
11. Papanicolaou GD, McCabe SJ, Firrell J. The prevalence and characteristics of nerve compression symptoms in the general population. J Hand Surg [Am]. 2001;26(3):460–6.
12. Richman JA, Gelberman RH, Rydevik B, et al. Carpal tunnel volume determination by magnetic resonance imaging three-dimensional reconstruction. J Hand Surg [Am]. 1987;12(5 Pt 1):712–7.
13. Skie M, Zeiss J, Ebraheim NA, et al. Carpal tunnel changes and median nerve compression during wrist flexion and extension seen by magnetic resonance imaging. J Hand Surg [Am]. 1990;15 (6):934–9.
14. Yoshioka S, Okuda Y, Tamai K, et al. Changes in carpal tunnel shape during wrist joint motion. MRI evaluation of normal volunteers. J Hand Surg [Br]. 1993;18(5):620–3.
15. Pacek CA, Chakan MC, Goitz RJ, Kaufmann RA, Li ZM. A morphological study of the transverse carpal ligament. Hand. 2009. doi:10.1007/s11552-009-9219-2